Synthesis and characterization of micron-size pyrite crystals

Rong Wu[a] and Ji-kang Jian
Department of Physical Science and Technology, XinJiang University, Urumqi, Xinjiang 830046, China and Central for Material Research, XinJiang University, Urumqi, Xinjiang 830046, China

Le-tian Tao and Yan-long Bian
Department of Physical Science and Technology, XinJiang University, Urumqi, Xinjiang 830046, China

Jin Li and Yan-fei Sun
Department of Physical Science and Technology, XinJiang University, Urumqi, Xinjiang 830046, China and Central for Material Research, XinJiang University, Urumqi, Xinjiang 830046, China

Jun Wang and Xing-Yan Zeng
Department of Physical Science and Technology, XinJiang University, Urumqi, Xinjiang 830046, China

(Received 30 December 2009; accepted 2 May 2010)

Mixed solvent of ethanol and water using $FeSO_4 \cdot 7H_2O$ and $(NH_2)_2CS$ as precursors with polyvinylpyrrolidone as surfactant was used to synthesize cubic FeS_2 (pyrite) crystals. Crystalline phase and surface morphologies of the crystals were characterized by X-ray diffraction and scanning electron microscopy, respectively. Volume ratio of solvent, reaction temperature, reaction time, and sulfur source were found to be the key parameters for the formation of pure pyrite crystals. Optimal micron-size pyrite crystals were successfully grown from a mixed solvent of ethanol and water with a volume ratio of 3:2, heated to a reaction temperature of 180 °C, and maintained for 36 h with thiourea as the sulfur source. © *2010 International Centre for Diffraction Data.* [DOI: 10.1154/1.3478339]

Key words: pyrite, FeS_2, solvothermal method, XRD, SEM

I. INTRODUCTION

Transition metal chalcogenides have been extensively studied for their applications in photovoltaic devices. The pyrite of iron disulfide (FeS_2) is of particular interest and shows promise for solar energy conversion devices in both photoelectrochemical and solid-state solar cells due to its favorable solid-state properties (Schröder *et al.*, 1999; Chen and Fan, 2001; Nath *et al.*, 2003; Velásquez *et al.*, 2005; Feng *et al.*, 2007). Large variety of techniques has been used in its preparation, such as thermal sulfuration of iron or oxides (de las Heras *et al.*, 1993; Heras *et al.*, 1996), flash evaporation (Ferrer and Scancez,1991), electrodeposition (Nakamura and Yamamoto, 2001), and metal organic chemical vapor transport (Tomas and Cibik,1998).

During the past decades, the solvothermal technique is becoming one of the most important tools for advanced material processing, particularly owing to its advantages in the production of nanostructural materials. Actually hydrothermal and solvothermal methods have been widely used to prepare chalcogenides. Chen *et al.* (2005a) reported the successful synthesis of cubic FeS_2 crystallites via a single-source approach using iron diethyldithiocarbamate as precursor under hydrothermal conditions. Gao *et al.* (2006) employed a novel hyposulfite self-decomposition route to produce semiconductor FeS_2 nanowebs. Recently Ni-, Co-, and As-doped pyrites have attracted much interest for the half-metallic properties due to fundamental physics in spintronics and potential application in spin-electronic devices (Abd El Halim *et al.*, 2002; Lehner *et al.*, 2006; Díaz-Chao *et al.*, 2008). Considerable progress has also been made by our group, which includes a single-stage low-temperature hydrothermal synthesis pyrite by using $FeSO_4$, $Na_2S_2O_3$, and S powder (Wu *et al.*, 2004b), solvothermal synthesis of nanocrystalline FeS_2 (Chen *et al.*, 2005b), and pyrite films prepared via sol-gel hydrothermal method combined with electrophoretic deposition (Duan *et al.*, 2004b)). At the same time, the so-called pyrites MX_2 (M=Ni, Fe, Co, Ni; X=S, Se) have been prepared in different acid and alkaline environment by hydrothermal and solvothermal methods (Wu *et al.*, 2004a; Duan *et al.*, 2004a). We have investigated the influence of reaction parameters such as different solvents, temperature, time, environment, and various systems. However, some questions remain. For example, though the hydrothermal and solvothermal methods can also control the products properties, the effects of the proportion of mixed solvent on the products are still unknown. Based on above progress, in this study we investigated solvothermal method for the preparation of pyrite using various mixed solvents of water and ethanol as well as S sources.

II. EXPERIMENTAL

All reagents were of analytical grade and were used as received without further purification. In a typical synthesis, 2 mmol of thiourea $[(NH_2)_2CS]$ and 1 g of polyvinylpyrrolidone (PVP) were dissolved in the mixed solvent of ethanol and water with a certain volume ratio (total volume=30 ml). The mixture was magnetically stirred for 15 min, then 1 mmol of iron sulphate $[FeSO_4 \cdot 7H_2O]$ was added into the solution and stirred for 10 min before being transferred into a Teflon-lined autoclave with 40 ml capacity. After being sealed, the autoclave maintained a fixed reaction temperature

[a]Author to whom correspondence should be address. Electronic mail address: rongwu1022@163.com

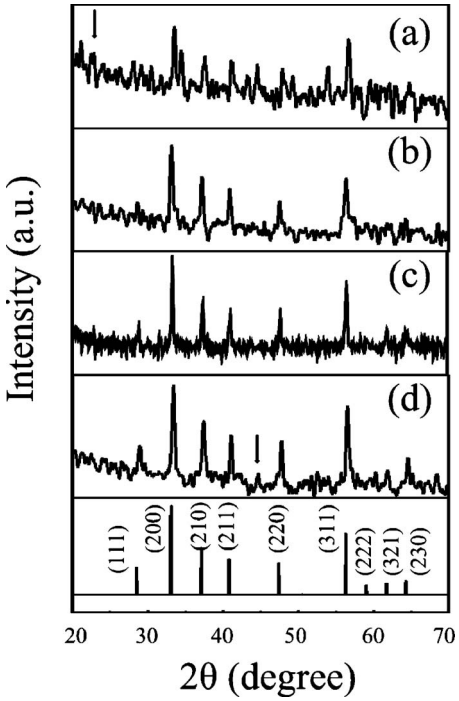

Figure 1. XRD patterns of the products obtained at 180 °C for 36 h with (a) distilled water and mixed solvents of ethanol and water with ratios of (b) 2:3, (c) 3:2, and (d) 4:1.

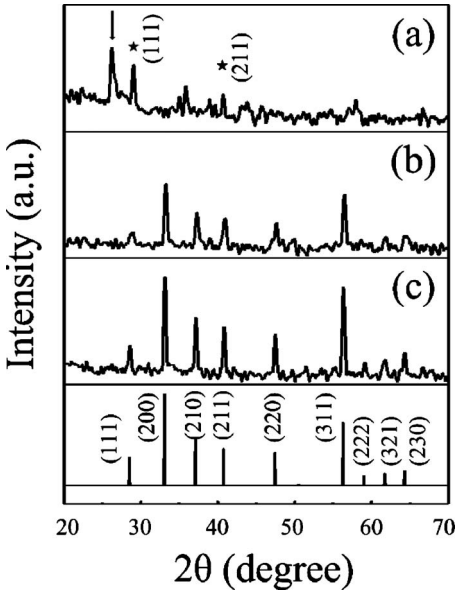

Figure 2. XRD patterns of the products obtained at (a) 120 °C, (b) 150 °C, and (c) 180 °C and maintained 36 h in a mixed solvent of ethanol and water with a volume ratio of 3:2.

in the range between 120 and 180 °C and a fixed reaction time between 12 and 48 h and then cooled to room temperature naturally. After reaction, the precipitates were collected, washed with carbon disulfide (CS_2), anhydrous ethanol, and distilled water several times to remove by-product, and then dried at 60 °C for 6 h in vacuum. Several sets of experiment were carried out to investigate the effects of reaction temperature, reaction time, volume ratio of the mixed solvent, and sulfur source.

The crystal phases of the products were examined by X-ray diffraction (XRD) using a Japan Mac science X-ray diffractionmeter with Cu $K\alpha$ radiation ($\lambda = 0.154\,06$ nm). Experimental conditions were 40 kV, 200 mA, $2\theta/\theta$ scan with $0.02°2\theta$ step, and a diffracted-beam graphite monochromator. Scanning electron microscopy (SEM) images were obtained by a field emission scanning electron microscopy (German leo1430vp), and an energy dispersive X-ray (EDX) analysis was also performed.

III. RESULTS AND DISCUSSION

A. Effect of volume ratio of solvents

Solvothermal synthesis in a mixed solvent usually involves two or more solvent components for a better control of crystal growth. Pure water and mixed solvents of ethanol and water with ratios of 2:3, 3:2, and 4:1 were used in this study. XRD patterns of four products obtained at 180 °C for 36 h with mixed solvents of different volume ratios are shown in Figure 1. Figure 1(a) is the XRD pattern obtained from the product synthesized from distilled water. The observed broad and weak pyrite (200), (210), (211), (220), and (311) peaks indicate that the pyrite phase is poorly crystalline. The presence of several other very broad and weak impurity peaks including a possible peak at $22.5°2\theta$ marked by an arrow in Figure 1(a) suggests that the product may also contain other impurity phase(s). The XRD pattern of the synthesized product obtained from solvent with the volume ratio of 2:3 is shown in Figure 1(b), and it indicates that the product is pure cubic FeS_2 with pyrite diffraction peaks of (200), (210), (211), (220), and (311). No impurity peaks are detected. Further increasing the volume ratio of ethanol and water to 3:2, sharp pyrite diffraction peaks of (111), (200), (210), (211), (220), (311), (321), and (230) can clearly be observed [see Figure 1(c)], indicating that the pyrite crystals are well crystallized. The lattice parameter of cubic FeS_2 determined from the observed diffraction peaks shown in Figure 1(c) is $a = 5.4180$ Å, which is in good agreement with that reported in PDF 42-1340. Figure 1(d) shows XRD pattern for the case with the solvent ratio of 4:1. The pyrite diffraction peaks are slightly broader and an impurity peak appears at about $45°2\theta$ [see the arrow in Figure 1(d)].

The above results suggest that ethanol restrains the formation of impurity phase(s), and the optimum volume ratio of ethanol to water for synthesizing a pure pyrite phase is 3:2.

B. Effect of reaction temperature

The effect of three reaction temperatures at 120, 150, and 180 °C with a reaction time of 36 h and a volume ratio between ethanol and water of 3:2 on crystal growth of pyrite was studied, and their XRD patterns are shown in Figure 2. For the case of the reaction at 120 °C, very weak XRD pattern was obtained [see Figure 2(a)]. The first diffraction peak located at about $26°2\theta$ is the diffraction of the orthorhombic FeS_2 marcasite [PDF 37-475, and see the arrow in Figure 2(a)], and the second and the third peaks [see the star in Figure 2(a)] can be identified to be the pyrite (111) and (211) peaks. The results indicate that the FeS_2 powder synthesized at 120 °C consists of both the cubic pyrite phase

https://doi.org/10.1154/1.3478339 Published online by Cambridge University Press

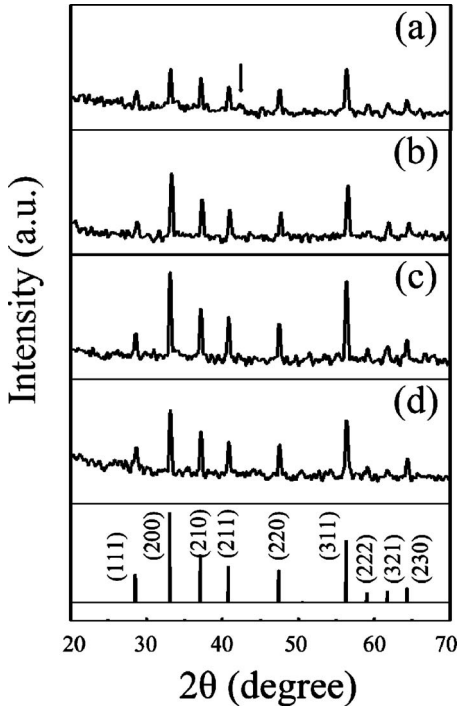

Figure 3. XRD patterns of the products maintained (a) 12 h, (b)24 h, (c) 36 h, and (d) 48 h and heated to 180 °C in a mixed solvent of ethanol and water with a volume ratio of 3:2.

and the orthorhombic marcasite phase of FeS_2. The XRD pattern for the product synthesized at 150 °C is plotted in Figure 2(b), showing eight pyrite peaks: (111), (200), (210), (211), (220), (311), (321), and (230). The pyrite (222) peak is hardly visible and the marcasite peak at about 26°2θ can no longer be detectable. Figure 2(c) depicts the strong XRD pattern for the product obtained at 180 °C, showing all nine pyrite peaks including the (222) peak.

The above results show that the processing temperature plays an important role in the formation of pure pyrite phase of FeS_2, and the optimum reaction temperature for synthesizing of a pure pyrite phase with good crystallinity is 180 °C.

C. Effect of reaction time

The effect of four reaction times of 12, 24, 36, and 48 h with a reaction temperature at 180 °C and a volume ratio between ethanol and water of 3:2 on crystal growth of pyrite was also studied, and their XRD patterns are depicted in Figure 3. It shows that the main pyrite phase for the 12 h product has broad and weak peaks, and a very broad and small weak impurity peak can be observed at 43°2θ [see the arrow in Figure 3(a)]. This impurity peak can no longer be detectable in the XRD patterns of the 24, 36, and 48 h products. The intensities of the pyrite diffraction peaks increase with increasing reaction time from 12 to 24 h [see Figure 3(b)], and the most intensive set of pyrite peaks was obtained for the case of 36 h reaction time [see Figure 3(c)]. The intensities of the pyrite diffraction peaks do not increase further but decrease when the reaction temperature was increased from 36 to 48 h [see Figure 4(d)].

Comparing Figures 2 and 3, the effect of reaction temperature on crystallinity is more obvious than that of reaction time. Crystal growth can also be controlled by the pressure in the sealed solvothermal system. In such a system, temperature, liquid volume, and vapor pressure are usually increased so as to increase the velocity of crystal growth. The commutative transition of liquid and vapor reaches a dynamic equilibrium when the temperature is sufficiently high, and the liquid-vapor interface is vanished so that pressure does not have an obvious effect on crystal growth (Chen *et al.*, 2005c). On the other hand, when the temperature reach a constant, crystal growth will be determined by the pressure brought by the reaction time. Finally, a new liquid-vapor dynamic equilibrium approaches and growth speed rate is constant or decreased.

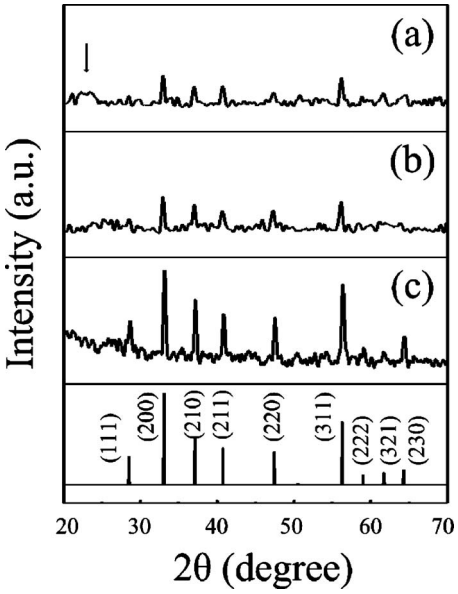

Figure 4. XRD patterns of the products obtained with (a) S powder, (b) sodium thiosulfate, and (c) thiourea as sulfur source at optimal reaction conditions.

D. Effect of sulfur source

The effect on as-prepared products synthesized using three different sulfur sources (namely, sulfur powder, sodium thiosulfate, and thiourea) with optimal synthesis conditions (i.e., solvent ratio of 3:2, reaction temperature of 180 °C, and reaction time of 36 h) is shown in Figure 4. For the case of using pure S powder as the sulfur source, the XRD pattern has weak pyrite peaks and a broad impurity peak at about

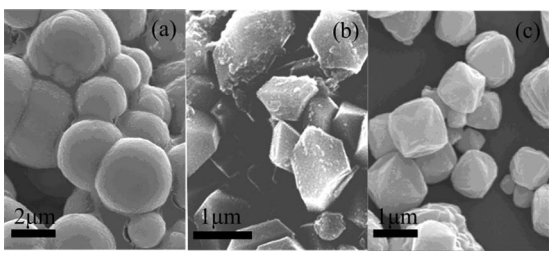

Figure 5. SEM images of the products obtained with (a) S powder, (b) sodium thiosulfate, and (c) thiourea as sulfur source at optimal reaction conditions.

https://doi.org/10.1154/1.3478339 Published online by Cambridge University Press

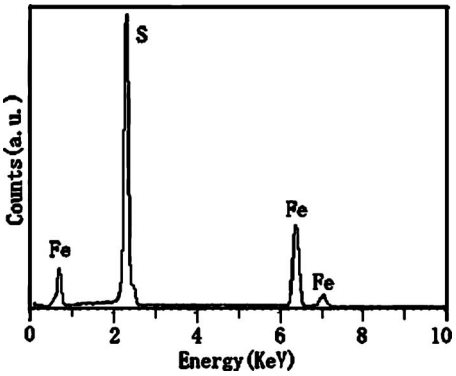

Figure 6. EDX spectrum of the optimal pyrite product.

22.5° 2θ [see Figure 4(a)]. The broad impurity peak at about 22.5° 2θ is no longer detectable for the case of using sodium thiosulfate ($Na_2S_2O_3$) as the sulfur source [see Figure 4(b)]. Pure pyrite powder with narrow pyrite peaks was obtained when thiourea was used as the sulfur source [see Figure 4(c)].

The XRD results show that thiourea can promote crystal growth of pyrite and inhibit other impurities, and the optimum sulfur source for synthesizing a pure pyrite phase with good crystallinity is thiourea.

Figure 5 shows the SEM images of pyrite crystals synthesized by the three sulfur sources, and differences in surface morphology of the three products can clearly be seen. As shown in Figure 5(a), the product made from the sulfur source of S powder consists of spherical grains and the sizes of the grains are about 1 to 2 μm. No obvious crystal facet can be observed. The observed surface morphology suggests that there were no sufficient island-coalescence processes during grain growth. The product used sodium thiosulfate as the sulfur source is composed of anomalous polyhedral crystals, and the crystals are characterized by distinct micron-size crystal facets [see Figure 5(b)]. As shown in Figure 5(c), the product used thiourea as the source consists of crystals with relatively clearly polyhedral shapes with sizes of about 1 μm or less. The product was also analyzed by EDX, and the elemental results confirm the presence of Fe and S in the product (see Figure 6).

All morphological features observed from the SEM images are consistent with the XRD results, and both show that the product with thiourea as the source has optimal crystallinity. Compared with XRD and SEM of three products, the conglobation effect of the S powder accelerates product glomeration during growth and aggregation process, while thiourea [$(NH_2)_2CS$] dissolves in the mixed solvents and releases S ions step by step so that the pyrite crystals can be adhered to the nuclei of the crystals and develop polyhedron grains. It should be noted that PVP was added as surfactant to disperse the particle in liquid when pyrite grains went through nucleation, growth, coalescence, and cluster progress.

IV. CONCLUSION

The results obtained in this study show that optimal micron-size pure pyrite crystals can be grown from a mixed solvent of ethanol and water with a volume ratio of 3:2, heated to a reaction temperature of 180 °C, and maintained for 36 h with PVP as surfactant. The SEM images are consistent with the XRD results, and both show that the product with thiourea as the source has optimal crystallinity.

ACKNOWLEDGMENTS

This work was supported by National Natural Science Foundation of China (Grant Nos. 10864004 and 50862008), Xinjiang University starting fund (Grant No. BS080109), National Innovation Experiment Program for University Students (Grant No. 081075503), and Key Project of College Scientific Research Projects of Xinjiang Uygur Autonomous Region (Grant No. XJEDU2008I05). The authors also thank the open fund of Surface Physics Laboratory (National Key Laboratory), Fudan University, China.

Abd El Halim, A. M., Fiechter, S. H., and Tributsch, G. (**2002**). "Control of interfacial barriers in *n*-type FeS_2 (pyrite) by electrodepositing metals (Co, Cu) forming isostructural disulfides," Electrochim. Acta **47**, 2615–2623.

Chen, X. and Fan, R. (**2001**). "Low-temperature hydrothermal synthesis of transition metal dichalcogenides," Chem. Mater. **13**, 802–5.

Chen, X. Y., Wang, Z. H., Wang, X., Wan, J. X., Liu, J. W., and Qian, Y. T. (**2005a**). "Single-source approach to cubic FeS_2 crystallites and their optical and electrochemical properties," Inorg. Chem. **4**, 951–954.

Chen, Y. H., Zheng, Y. F., Zhang, X. G., Sun, Y. F., and Dong, Y. Z. (**2005b**). "Solvothermal synthesis of nanocrystalline FeS_2," Sci. China, Ser. G **48**, 188–200.

Chen, Y. H., Zheng, Y. F., Zhang, X. G., Sun, Y. F., and Dong, Y. Z. (**2005c**). "Effect of pH value on FeS_2 powder synthesized by solvothermal process," Acta Physico-Chimica Sinica **21**, 419–424.

De las Heras, C., Ferrer, I. J., and Scancez, C. (**1993**). "Pyrite tin films: Improvement in their optical and electrical properties by annealing at differential temperature in sulfur atmosphere," J. Appl. Phys. **74**, 4551–4556.

De las Heras, C., Martin, J. L., and Vidals, D. (**1996**). "Structural and microstructural features of pyrite FeS_{2-x} thin films obtained by thermal sulfuration of iron," J. Mater. Res. **11**, 211–214.

Díaz-Chao, P., Ferrer, I. J., and Sánchez, C. (**2008**). "Co distribution through *n*-type pyrite thin films," Thin Solid Films **516**, 7116–7119.

Duan, H., Zheng, Y. F., Dong, Y. Z., Zhang, X. G., and Sun, Y. F. (**2004a**). "Pyrite (FeS_2) films prepared via sol-gel hydrothermal method combined with electrophoretic deposition (EPD)," Mater. Res. Bull. **39**, 1861–1868.

Duan, H., Zheng, Y. F., Dong, Y. Z., and Sun, Y. F. (**2004b**). "Nanocrystalline pyrite cobalt disulfide synthesized by solvent-thermal preparation," Chin. J. Mech. Eng. **28**, 49–51.

Feng, X., He, X. M., Pu, W. H., Jiang, C. Y., and Wan, C. R. (**2007**). "Hydrothermal synthesis of FeS_2 for lithium batteries," Ionics **13**, 375–377.

Ferrer, I. J. and Scancez, C. (**1991**). "Characterization of FeS_2 tin films prepared by thermal sulfidation of flash evaporated iron," J. Appl. Phys. **70**, 2641–2647.

Gao, P., Xie, Y., Ye, L., Chen, Y., and Guo, Q. X. (**2006**). "From 2D nanoflats to 2D nanowire networks: A novel hyposulfite self-decomposition route to semiconductor FeS_2 nanowebs," Cryst. Growth Des. **6**, 583–587.

Lehner, S. W., Savage, K. S., and Ayers, J. C. (**2006**). "Vapor growth and characterization of pyrite (FeS2) doped with Co, Ni and As: Variations in semi conducting properties," J. Cryst. Growth **286**, 306–317.

Nakamura, S. and Yamamoto, A. (**2001**). "Electrodeposition of pyrite tin films for potovoltaic cells," Sol. Energy Mater. Sol. Cells **65**, 79–85.

Nath, M., Choudhur, A., Kundu, A., and Rao, C. N. R. (**2003**). "Synthesis and characterization of magnetic ion sulfide nanowires," Adv. Mater. **15**, 2098–2101.

Schröder, D., Kretzschmar, I., and Schwarz, H. (**1999**). "On the structural dichotomy of cationic, anionic, and neutral FeS_2," Inorg. Chem. **38**, 3474–3480.

Tomas, B. and Cibik, B. (**1998**). "Formation of secondary iron-sulfur phase during the growth of polycrystalline iron pyrite tin films by MOCVD," J. Mater. Sci. **9**, 61–64.

Velásquez, P., Leinen, D., Pascual, J., Ramos-Barrado, J. R., Grez, P., Gómez, H., Schrebler, R., Del Río, R., and Córdova, R. (**2005**). "A chemical, morphological, and electrochemical (XPS, SEM/EDX, CV, and EIS) analysis of electrochemically modified electrode surfaces of natural chalcopyrite ($CuFeS_2$) and pyrite (FeS_2) in alkaline solutions," J. Phys. Chem. B **109**, 4977–4988.

Wu, R., Zheng, Y. F., Zhang, X. G., Sun, Y. F., Xu, J. B., and Jian, J. K. (**2004a**). "Hydrothermal synthesis and crystal structure of pyrite," J. Cryst. Growth **266**, 523–527.

Wu, R., Zheng, Y. F., Zhang, X. G., Sun, Y. F., Xu, J. B., and Jian, J. K. (**2004b**). "EDTA-assisted hydrothermal syntheses of $FeS_2/NiSe_2$ nanocomposites and the optical and electrical properties of their thin films," Acta Phys. Sin. **10**, 3493–3496.

https://doi.org/10.1154/1.3478339 Published online by Cambridge University Press